Article

WT1 Mutants Reveal SRPK1 to Be a Downstream Angiogenesis Target by Altering VEGF Splicing

Elianna M. Amin,[1,2] Sebastian Oltean,[2] Jing Hua,[2] Melissa V.R. Gammons,[2] Maryam Hamdollah-Zadeh,[2] Gavin I. Welsh,[3] Man-Kim Cheung,[1] Lan Ni,[3] Satoru Kase,[4] Emma S. Rennel,[2] Kirsty E. Symonds,[2] Dawid G. Nowak,[2] Brigitte Royer-Pokora,[5] Moin A. Saleem,[3] Masatoshi Hagiwara,[6] Valérie A. Schumacher,[5,7,8] Steven J. Harper,[2] David R. Hinton,[4] David O. Bates,[2,9,*] and Michael R. Ladomery[1,9,*]

[1]Centre for Research in Biomedicine, Faculty of Health and Life Sciences, University of the West of England, Coldharbour Lane, Bristol BS16 1QY, UK
[2]Microvascular Research Laboratories, Bristol Heart Institute, School of Physiology and Pharmacology, University of Bristol, Preclinical Veterinary Sciences Building, Southwell Street, Bristol BS2 8EJ, UK
[3]Academic and Children's Renal Unit, Lifeline Building, Southmead Hospital, University of Bristol, Bristol BS10 5NB, UK
[4]Department of Pathology, Keck School of Medicine, University of Southern California, 1355 San Pablo Street, Los Angeles, CA 90089-9092, USA
[5]Institute of Human Genetics and Anthropology, Heinrich Heine University, Medical Faculty, Duesseldorf 40225, Germany
[6]Department of Anatomy and Developmental Biology, Graduate School of Medicine, Kyoto University, Kyoto 606-8501, Japan
[7]Department of Medicine, Children's Hospital Boston, Boston, MA 02115, USA
[8]Department of Pediatrics, Harvard Medical School, Boston, MA 02115, USA
[9]These authors contributed equally to this work
*Correspondence: Dave.Bates@bris.ac.uk (D.O.B.), Michael.Ladomery@uwe.ac.uk (M.R.L.)
DOI 10.1016/j.ccr.2011.10.016

SUMMARY

Angiogenesis is regulated by the balance of proangiogenic $VEGF_{165}$ and antiangiogenic $VEGF_{165}b$ splice isoforms. Mutations in *WT1*, the Wilms' tumor suppressor gene, suppress $VEGF_{165}b$ and cause abnormal gonadogenesis, renal failure, and Wilms' tumors. In *WT1* mutant cells, reduced $VEGF_{165}b$ was due to lack of WT1-mediated transcriptional repression of the splicing-factor kinase SRPK1. WT1 bound to the *SRPK1* promoter, and repressed expression through a specific WT1 binding site. In *WT1* mutant cells SRPK1-mediated hyperphosphorylation of the oncogenic RNA binding protein SRSF1 regulated splicing of VEGF and rendered *WT1* mutant cells proangiogenic. Altered VEGF splicing was reversed by wild-type WT1, knockdown of SRSF1, or SRPK1 and inhibition of SRPK1, which prevented in vitro and in vivo angiogenesis and associated tumor growth.

INTRODUCTION

Tumor growth requires new vessel formation, and this is driven predominantly by VEGF, the most potent angiogenic molecule known and the principal target for antiangiogenic therapy (Hurwitz et al., 2004). VEGF is alternatively spliced to form two families, one by splicing to a proximal 3′ splice site in exon 8 (Houck et al., 1991), and a second by splicing to a distal 3′ splice site in exon 8 (Bates et al., 2002; Cébe Suarez et al., 2006; Woolard et al., 2004). Whereas proximal splice-site (PSS) selection results in angiogenic isoforms of VEGF, including $VEGF_{165}$, distal splice-site (DSS) selection results in a family with antiangiogenic properties (e.g., $VEGF_{165}b$; see Figure S1A available online). $VEGF_{165}b$ inhibits VEGFR2 signaling by inducing differential phosphorylation (Kawamura et al., 2008) and intracellular trafficking (Ballmer-Hofer et al., 2011), and it blocks angiogenesis in vivo in the mouse dorsal skin and chick chorioallantoic membrane (Cébe Suarez et al., 2006), rabbit

Significance

Regulation of angiogenesis is critical for tumor growth. This is regulated by the proangiogenic VEGF isoforms. Antiangiogenic isoforms, formed by alternative splicing, are found in normal, healthy tissues and are downregulated in many tumors. Here, we identify a link between mutations in a tumor suppressor gene and regulators of angiogenesis. This link, through transcriptional regulation of a splicing-factor kinase indicates that (1) WT1 regulates splicing through repression of SRPK1, (2) SRPK1 may be a target for antiangiogenic therapy, and (3) alternative splicing in tumors under genetic as well as environmental control can regulate tumor growth. These results provide a pathway linking two mechanisms known to be altered in cancer—angiogenesis and alternative splicing.

cornea and rat mesentery (Woolard et al., 2004), developing rat ovary (Artac et al., 2009) and testis (Baltes-Breitwisch et al., 2010), melanoma, prostate, renal, and colon cancer (Varey et al., 2008), sarcoma, and metastatic melanoma(Rennel et al., 2008), and in the mouse retina and choroid (Hua et al., 2010; Konopatskaya et al., 2006). The second member of the family so far investigated, $VEGF_{121}b$ is also antiangiogenic in the retina and in colon cancer (Rennel et al., 2009). The role of the antiangiogenic family has not yet been investigated in as much detail as the angiogenic family, although it appears to be relatively highly expressed in nonangiogenic tissues (Woolard et al., 2009) and is downregulated during angiogenesis (Bates et al., 2002; Perrin et al., 2005; Varey et al., 2008). $VEGF_{165}b$ is downregulated in the mammary gland during pregnancy, when vascular remodelling and angiogenesis are required for epithelial gland formation. Overexpression of $VEGF_{165}b$ in the mammary gland during pregnancy inhibits duct formation, resulting in reduced milk formation and pup starvation (Qiu et al., 2008), and inhibition of endogenous $VEGF_{165}b$ in the ovary results in abnormal angiogenesis and increased follicle progression (Artac et al., 2009). In the kidney, expression of $VEGF_{165}b$ in the podocyte controls permeability in the kidney and maintains normal glomerular filtration rates by regulating fenestral formation (Qiu et al., 2010).

As $VEGF_{165}b$ and $VEGF_{165}$ are generated from the same transcript, the relative amount of the proangiogenic versus antiangiogenic isoforms is dependent upon splicing to either the PSS (angiogenic $VEGF_{165}$) or the DSS (antiangiogenic $VEGF_{165}b$) (Harper and Bates, 2008). The control of this splicing is poorly understood, but recent studies have identified the role of three key serine-arginine-rich (SR) proteins, SRSF6 (SRp55) (Manetti et al., 2011; Nowak et al., 2008), SRSF1 (ASF/SF2) (Nowak et al., 2010), and SRSF2 (SC35) (Merdzhanova et al., 2010), in the control of the terminal splice-site selection. SRSF1 has been implicated in proximal splice-site selection, induced by IGF-1, and binding to the region around the PSS. SRSF6 has been implicated in distal splice-site selection as it binds around the DSS and is upregulated by TGFβ1 in systemic sclerosis, resulting in increased $VEGF_{165}b$ expression and inhibition of angiogenesis (Manetti et al., 2011). A key study by Schumacher et al. in 2007 identified a lack of the antiangiogenic isoform in laser-dissected glomeruli of Denys Drash Syndrome (DDS) patients with a genetic mutation in the Wilms' tumor suppressor gene WT1 (Schumacher et al., 2007). These patients have increased risk of Wilms' tumors, intersex disorders, and renal failure (Denys et al., 1967; Drash et al., 1970). Wilms' tumors are highly vascularized tumors with high VEGF levels (Blann et al., 2001; Sköldenberg et al., 2001), and WT1 mutations or altered expression are also found in other highly vascularized tumors such as prostate cancer, hematological cancers, and colorectal, breast, desmoid and brain tumors (Hohenstein and Hastie, 2006). WT1 is also expressed as different isoforms by alternative splicing (Haber et al., 1991). The most widely studied isoforms are the inclusion or exclusion of exon 5 and an alternative splice donor site in exon 9, which encodes three amino acids, KTS. The -KTS isoforms interact preferentially with DNA. Thus, WT1 can be exon 5+ or exon 5− and KTS+ or KTS−, and all four isoforms are expressed in several tissues (Morrison et al., 2008). As DDS-causing mutations in WT1 can alter VEGF

splicing (Schumacher et al., 2007), we have investigated this link between WT1 and splicing of the VEGF transcript, testing the hypothesis that WT1 mutations regulate splicing through splice-factor-specific mechanisms.

RESULTS

DDS Cells Have Reduced Distal Splice-Site Selection in VEGF Resulting in Less $VEGF_{165}b$

Schumacher et al. have shown that laser-dissected glomeruli from patients with DDS lack $VEGF_{165}b$ (Schumacher et al., 2007). To determine whether this was reproduced in an in vitro cell system, we used the previously described conditionally immortalized cell line from a patient with a C1096T mutation in WT1 (Viney et al., 2007). This results in a single amino acid substitution at amino acid 366 from an arginine to a cysteine in the third zinc finger, critical for DNA binding. Figure 1A shows that whereas normal podocytes express both isoforms approximately equally, in the DDS podocytes the $VEGF_{165}$ isoform was dominant. To ensure that this was due to a lack of a functional WT1 gene, a stable DDS cell line was generated expressing wild-type WT1 (+exon5/−KTS; "rescued" DDS). This restored expression of $VEGF_{165}b$. To determine whether altered splicing resulted in altered $VEGF_{165}b$ protein levels, cells were lysed, protein extracted, and subjected to VEGF ELISA, using a pan-VEGF capture antibody and then either a pan-VEGF or a $VEGF_{165}b$ specific detection antibody. Figure 1B shows that DDS cells had increased $VEGF_{165}$, but decreased $VEGF_{165}b$. Rescued DDS cells restored overall VEGF expression and splicing toward normal podocyte levels. Quantitative PCR (qPCR) indicated no change in total VEGF mRNA levels between DDS ($0.10 \pm 0.01\%$ of GAPDH) and wild-type ($0.15 \pm 0.06\%$ of GAPDH) cell lines, and overexpression of wild-type WT1 (+/−) also resulted in no change in total VEGF expression ($0.13 \pm 0.01\%$). To confirm that this was $VEGF_{165}b$ and $VEGF_{165}$ being expressed, proteins were subjected to immunoblot. Figure 1C shows that it was the 165 amino acid isoform ($VEGF_{165}b$) that was altered. To determine whether podocytes from DDS patients with other mutations in WT1 also had altered $VEGF_{165}b$ expression, conditionally immortalized podocytes generated from patients with M342R or G349C mutations were used. Figure 1D shows that cells derived from both additional patients had reduced $VEGF_{165}b$ expression relative to normal podocytes. To determine whether WT1 was capable of altering expression in other cell types, HeLa cells (which normally express low levels of $VEGF_{165}b$) and HEK293T cells (which do express $VEGF_{165}b$) were examined. Figure 1E shows that transfection of HeLa cells with either $WT1^{-/-}$ (−exon5/−KTS) or $WT1^{+/-}$ (+exon5/−KTS) resulted in $VEGF_{165}b$ expression and reduced $VEGF_{165}$ expression, and in HEK293 cells this transfection resulted in increased $VEGF_{165}b$ and reduced $VEGF_{165}$. The presence or absence of WT1's exon 5 did not alter the effect, but the +KTS isoforms ($WT1^{-/+}$ and $WT1^{+/+}$) were unable to switch splicing to increase $VEGF_{165}b$ expression in either HeLa (Figure S1B) or HEK cells (Figure S1C). Splice-site selection in exon 9 (+KTS) of WT1 itself was not altered in DDS cells (Figure S1D). Thus, to our surprise, the splicing effect is limited to isoforms that lack the KTS sequence, isoforms that are mostly associated with stable DNA binding of its GC rich target
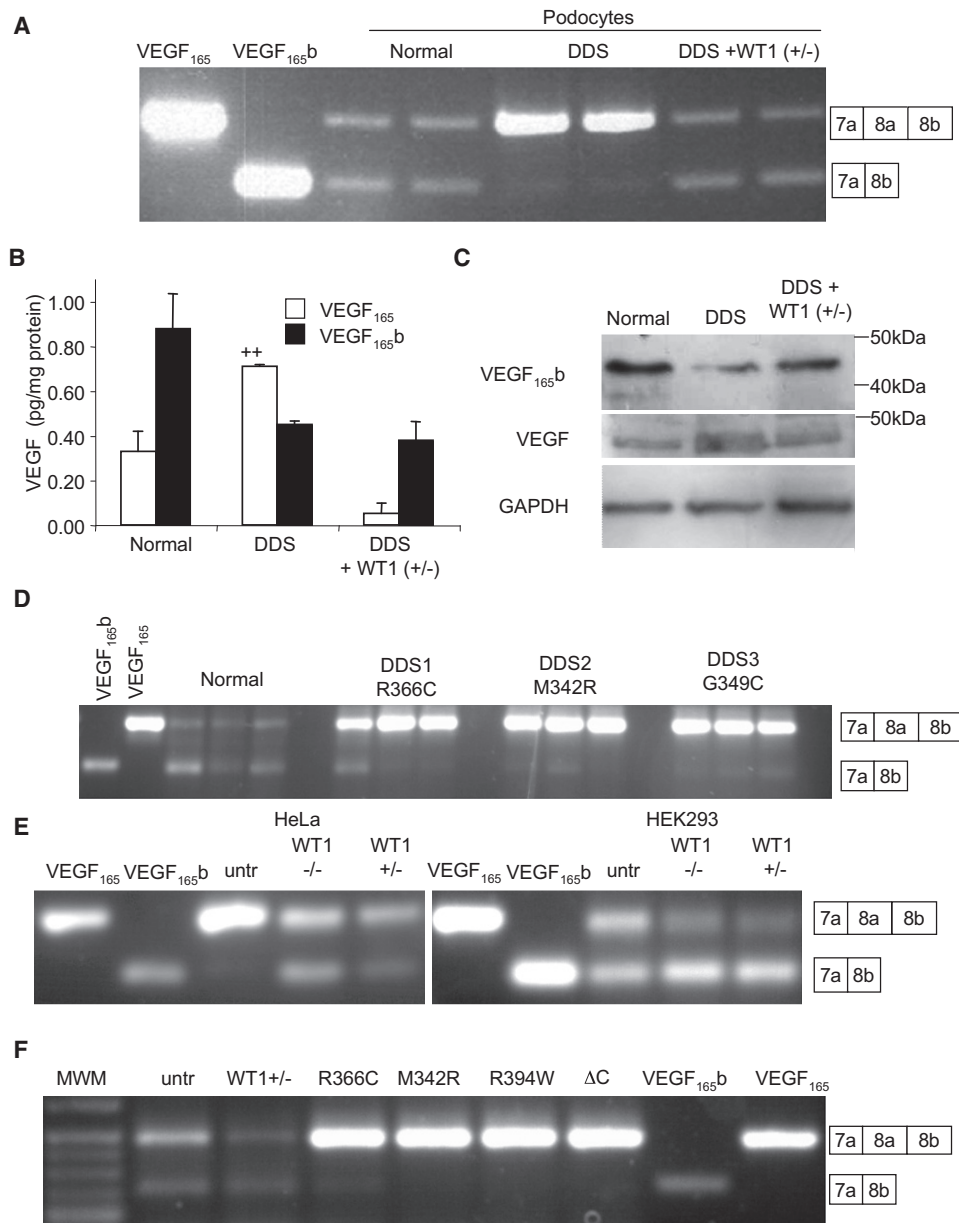
Figure 1. Wild-Type WT1 Induces Antiangiogenic VEGF$_{165}$b Expression

(A) RT-PCR of mRNA extracted from normal or *DDS* podocytes using primers that detect both proximal and distal splice isoforms of VEGF. VEGF$_{165}$ and VEGF$_{165}$b cDNAs are used as positive controls. Transfection of *DDS* podocytes with WT1 (+exon 5/−KTS) restored VEGF$_{165}$b splicing. Boxes indicate exon usage represented by the bands.

(B) ELISAs for VEGF$_{165}$b or VEGF$_{165}$ protein using a pan-VEGF capture antibody and specific detection antibodies. VEGF$_{165}$ was calculated from the difference between pan-VEGF and VEGF$_{165}$b.

(C) Immunoblot of protein extracted from normal podocytes, *DDS* podocytes, or *DDS* cells transfected with wild-type WT1(+/−) using antibodies to VEGF$_{165}$b, total VEGF or GAPDH.

(D) RT-PCR of podocyte cell lines (three replicates) from three different *DDS* patients with different WT1 mutations show reduced VEGF$_{165}$b expression.

(E) RT-PCR of mRNA from HeLa and HEK293 cells show expression of VEGF$_{165}$b in HEK293 but not HeLa cells (untr = untransfected), but both cell types have increased VEGF$_{165}$b expression in the presence of WT1 (−/−), and WT1 (+/−).

(F) Transfection of HEK293 cells with plasmids containing *DDS*-causing WT1 mutations abolished VEGF$_{165}$b expression. Wild-type WT1(+/−) overexpression increases distal splicing relative to proximally spliced isoforms. Bar charts are mean ± SEM. See also Figure S1.

sequence, suggesting it was not a direct RNA binding effect of WT1 but due to a transcriptional target of WT1. To determine whether other *DDS* mutations could alter splicing in HEK cells, we transfected HEK cells with WT1 containing the R366C, M342R, or R394W *DDS* mutations and a C-terminal deletion (Bor et al., 2006). All four mutations reduced VEGF$_{165}$b

expression relative to untransfected cells, whereas wild-type WT1(+/−) transfection increased the ratio of VEGF$_{165}$b to VEGF$_{165}$ (Figure 1F).

The Splice Factor SRSF1 Is Nuclear in *DDS* Podocytes and Regulates VEGF Splicing

We have previously shown that overexpression of splicing factor, arginine/serine-rich 1 (SRSF1, also called SFRS1, ASF, SF2, SF2/ASF, or ASF/SF2) results in increased VEGF$_{165}$ but not VEGF$_{165}$b (Nowak et al., 2008). To determine whether there was any alteration in SRSF1 expression, podocytes were stained with a goat polyclonal anti-SRSF1 antibody. In normal podocytes, SRSF1 was found in both the nucleus and the cytoplasm whereas in *DDS* cells it was localized predominantly in the nucleus. In rescued *DDS* cells, cytoplasmic localization of SRSF1 was restored (Figure 2A). To confirm this, cells were stained with a different mouse monoclonal SRSF1 antibody and similar staining was seen (Figure S2A). Staining of HeLa cells (no VEGF$_{165}$b expression) indicated nuclear staining of SRSF1, but HEK293 cells (VEGF$_{165}$b and VEGF$_{165}$ expression) showed both nuclear and cytoplasmic staining (Figure S2B), consistent with nuclear localization of SRSF1 predicting reduced VEGF$_{165}$b expression. To examine relative nuclear localization, a nuclear extract or whole-cell lysate from normal or *DDS* podocytes was subjected to immunoblotting with an anti-SRSF1 antibody. Figure 2B shows that whereas total SRSF1 protein expression (whole-cell lysate) is the same in *DDS* and normal podocytes, it is weakly localized in the nucleus in normal cells (intensity was 18 ± 6% of whole-cell lysate intensity) but strongly localized in the nucleus of *DDS* cells (95 ± 5%, N = 3). qPCR was carried out to confirm that there was no overall change in SRSF1 expression, which was not significantly different in *DDS* podocytes (0.12 ± 0.02% of GAPDH) compared with wild-type (0.23 ± 0.12%) or rescued (0.12 ± 0.01%) cells. SRSF1 is known to shuttle to the nucleus when phosphorylated (Sanford et al., 2005, 2008). To explore whether nuclear SRSF1 was phosphorylated in *DDS* podocytes, a high-resolution immunoblot of nuclear or cytoplasmic protein, untreated or treated with phosphatase, was carried out using two different SRSF1 antibodies. Figure 2C shows that whereas cytoplasmic SRSF1 was unaffected by phosphatase treatment, nuclear lysate treatment with phosphatase resulted in a lower-molecular-weight band. To then determine the phosphorylation status of SRSF1 after WT1 mutation, we immunoprecipitated protein from whole-cell lysate with an anti-SRSF1 antibody, then probed with a pan-phospho-SR protein antibody. Compared with normal podocytes (77 ± 2.5% of SRSF1 intensity) there was stronger phosphorylation of SRSF1 in *DDS* podocytes (87 ± 1.6%), and this was inhibited in the rescued *DDS* cells (71 ± 1%; Figure 2D). This was also seen when protein was immunoprecipitated with a phospho-SR protein and probed for SRSF1 (Normal 181 ± 7% of SRSF, *DDS* 244 ± 13%, rescued 163 ± 11%; Figure 2E). To determine whether nuclear SRSF1 was required for the inhibition of VEGF distal splicing a vector encoding nuclear-targeted SRSF1 (that fails to shuttle to the cytoplasm) was transfected into the podocytes. This resulted in complete inhibition of distal VEGF splicing (Figure 2F).

To determine whether SRSF1 was exhibiting greater splicing activity in *DDS* than normal podocytes, known targets of

SRSF1 were investigated. Mitogen-activated protein kinase signal-integrating kinase 2 (MNK2) is expressed as two splice isoforms, and SRSF1 overexpression has been shown to increase splicing of the MNK2b isoform (Karni et al., 2007). hnRNPA2/B1 is also alternatively spliced by SRSF1, with increased SRSF1 activity favoring inclusion of exon 2 to result in hnRNPB1 expression. MNK2 and hnRNPA2/B1 mRNA expression were investigated by RT-PCR. Figure 2G shows that *DDS* podocytes expressed the MNK2b isoform, whereas normal podocytes express MNK2a. The expression of MNK2b in rescued *DDS* cells once again reflected its splicing pattern in wild-type cells. Similarly, in *DDS* podocytes, hnRNPB1 was increased, and this was restored by rescue with WT1. In contrast Rac1b, another SRSF1 identified target (Gonçalves et al., 2009) was not altered in *DDS* (Figure S2C).

To determine whether SRSF1 was required for preferential proximal splicing of VEGF, *DDS* podocytes were transfected with three different siRNAs to SRSF1. qPCR for SRSF1 showed that this resulted in a reduction to 8.5 ± 4%, 15 ± 9.3%, and 15.8 ± 8.8% of SRSF1 mRNA expression in the scrambled siRNA transfected cells for siRNA1, 2, and 3, respectively. Figure 2H shows that all three siRNAs resulted in VEGF$_{165}$b expression. To ensure that this was not an off-target effect, cells were transfected with an SRSF1 construct resistant to siRNA1. This abolished the effect of siRNA1, again inhibiting VEGF$_{165}$b expression (Figure S2D). Overexpression of splice factors SRSF1, 2, 4–7 had minimal effect on VEGF$_{165}$b expression in HeLa cell, and overexpression of SRSF1–6 and SAM68 had no effect on *DDS* cells (Figure S2E).

SRPK1 Expression Is Elevated in Denys Drash Syndrome

SRSF1 nuclear localization is brought about by phosphorylation by a number of splicing factors, including SRPK1 (Zhong et al., 2009). To investigate whether SRPK1 might be involved, we measured SRPK1 mRNA levels in podocytes by qPCR. *DDS* podocytes showed a 15-fold increase in SRPK1 mRNA compared with normal podocytes (Figure 3A). This increase was significantly reduced in rescued *DDS* cells (p < 0.01, ANOVA). To identify whether SRPK1 protein levels were also altered, we subjected protein extracts from podocytes to immunoblotting using an SRPK1 antibody. Figure 3B shows that SRPK1 protein expression was increased in *DDS* cells (89 ± 23% of GAPDH) compared with normal podocytes (68 ± 22%), but not in rescued *DDS* cells (79 ± 23%). To determine whether SRPK1 activation could be affecting SRSF1 localization, we used a small molecule inhibitor of SRPK1, *N*-[2-(1-piperidinyl)-5-(trifluoromethyl)phenyl] isonicotinamide (SRPIN340) (Fukuhara et al., 2006). Treatment of *DDS* cells with 10 μM SRPIN340 or siRNA to SRPK1 resulted in relocalization of the SRSF1 to the cytoplasm (Figure 3C), as measured using a polyclonal goat antibody to SRSF1. This was confirmed with a monoclonal antibody to SRSF1 (Figure S3A).

SR Protein Kinase Inhibition Restores the Expression of Antiangiogenic VEGF

To identify whether SRPIN340 could affect alternative splicing of VEGF, cells were treated with 10 μM SRPIN340 and mRNA extracted and subjected to RT-PCR. Figure 3D shows that normal podocytes treated with SRPIN340 increased their
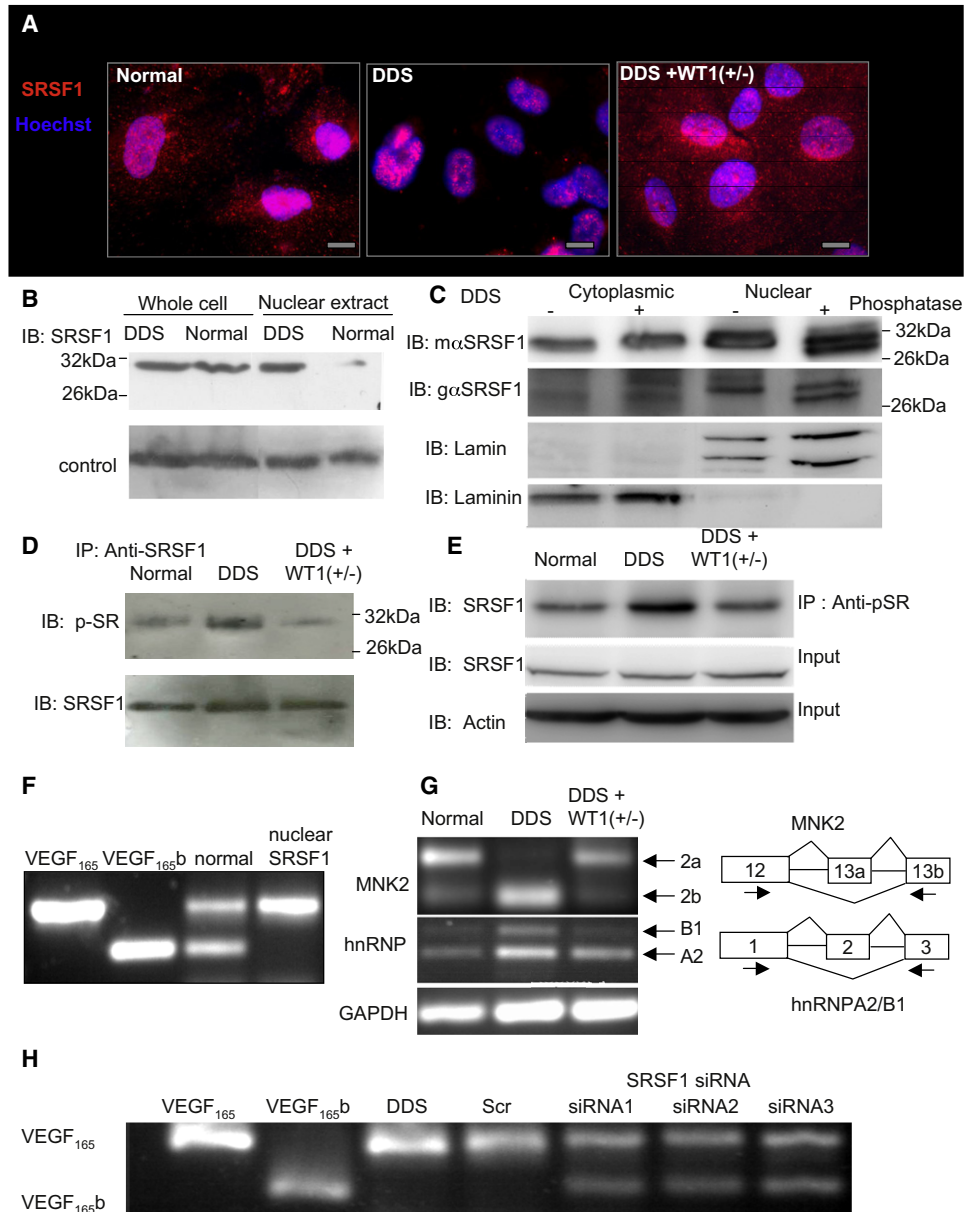
Figure 2. Mutant WT1 Induces Phosphorylation and Nuclear Localization of SRSF1, Which Regulates VEGF Splicing

(A) SRSF1 is absent from the cytoplasm when WT1 is mutated. Immunofluorescence staining of SRSF1 (red) of normal, *DDS* (R366C), and WT1-rescued *DDS* [*DDS*+WT1(+/−)] podocytes. Nuclei are counterstained blue. Scale bar = 10 μm.

(B) SRSF1 is more nuclearly localized in DDS than in normal podocytes. Protein was extracted from whole cells or from nuclear extracts of podocytes and subjected to immunoblotting for SRSF1.

(C) Nuclear SRSF1 is phosphorylated. Protein was extracted from flasks of *DDS* podocytes as either a cytoplasmic or a nuclear extract, and half-treated with phosphatase and subjected to high-resolution SDS PAGE and immunoblotting using mouse monoclonal (mαSRSF1) or goat polyclonal (gαSRSF1) antibodies to SRSF1, the cytoplasmic protein laminin, and the nuclear protein lamin.

(D) SRSF1 is hyperphosphorylated in DDS. Protein was extracted from podocytes, immunoprecipitated with an SRSF1 antibody, and immunoblotted with a pan-phospho SR antibody (top) or SRSF1 antibody (bottom).

(E) Protein was extracted from podocytes and half-immunoprecipitated with an anti-phosphoSR protein antibody. Both the IP and the crude protein extract were immunoblotted with an SRSF1 antibody and actin as a loading control.

(F) Nuclear localization of SRSF1 inhibits distal splicing. Normal podocytes were transfected with a vector encoding SRSF1 that fails to shuttle into the cytoplasm (nucleus-specific), and RNA was extracted and amplified for VEGF expression.

(G) Additional SRSF1 targets are alternatively spliced in DDS podocytes. RNA from normal or *DDS* podocytes was subjected to RT-PCR using exon spanning primers for the MNK2 cDNA (top) or hnRNPA2/B1 (middle) or GAPDH (bottom).

(H) Knockdown of SRSF1-induced VEGF$_{165}$b expression in DDS podocytes. *DDS* podocytes were transfected with scrambled siRNA (scr) or three different siRNAs to SRSF1 in the 3′UTR (siRNA1), in exons 2–3 (siRNA2) or exon 3 (siRNA3). See also Figure S2.
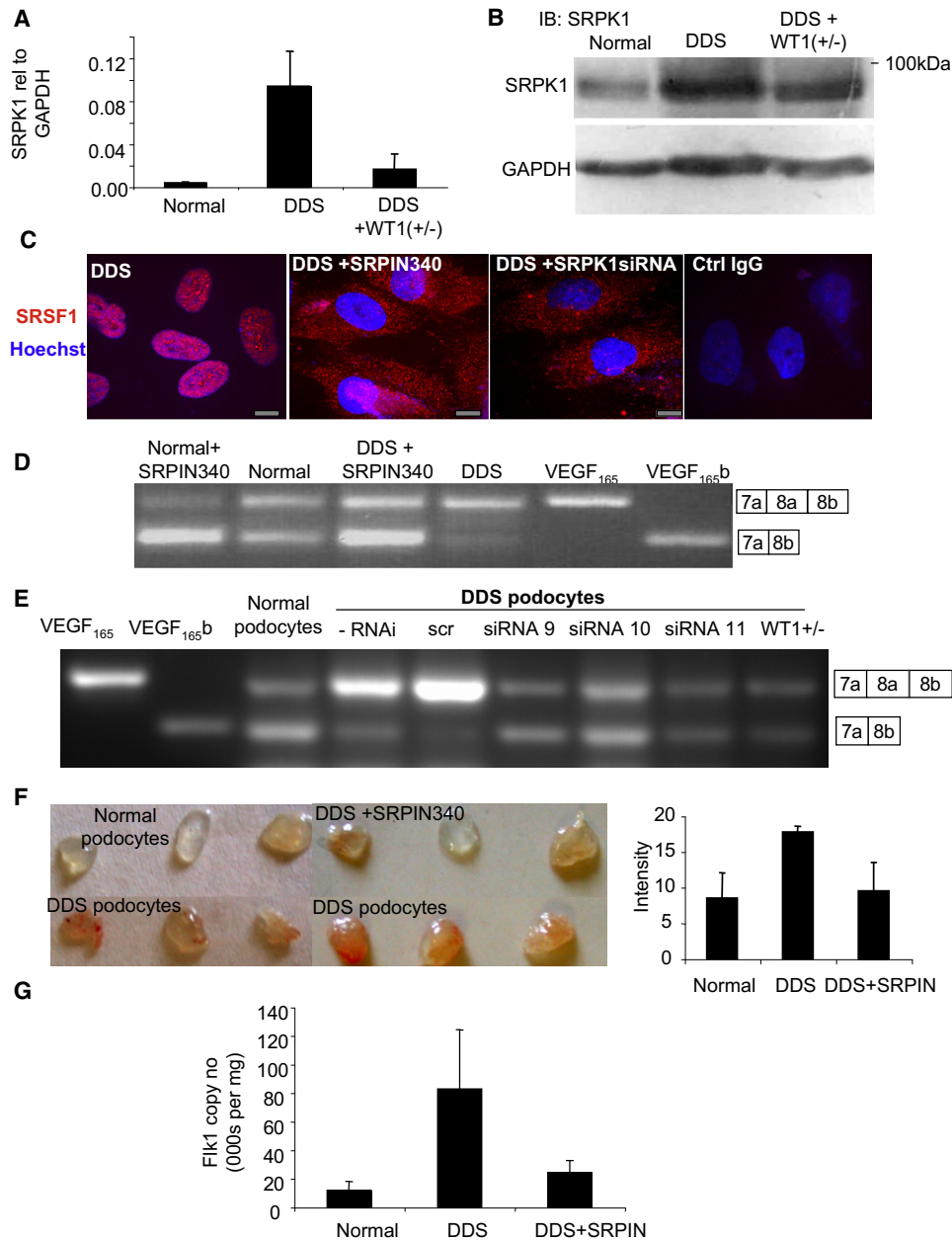
Figure 3. Increased SRPK1 Expression Increases SRSF1 Nuclear Localization and VEGF Proximal Splicing

(A) SRPK1 is upregulated in DDS podocytes. mRNA was extracted from normal, *DDS*, or rescued podocytes and subjected to qPCR using primers specific for SRPK1.

(B) SRPK1 protein is upregulated in DDS podocytes. Immunoblot (IB) using SRPK1 antibody in protein extracted from *DDS* podocytes, normal podocytes, and wild-type WT1(+/−) overexpressing podocytes.

(C) SRSF1 localization is SRPK1 dependent. Immunofluorescence for SRSF1 (red) is shown. *DDS* cells were treated with 10 μM of the SRPK1 inhibitor SRPIN340 or by knockdown of SRPK1 in *DDS* podocytes. Scale bar = 10μm.

(D) SRPK1 inhibition switches splicing to VEGF$_{165}$b. RT-PCR of mRNA extracted from normal or *DDS* podocytes untreated or treated with the SRPK1 inhibitor SRPIN340 using primers for VEGF$_{165}$ (top band) or VEGF$_{165}$b (lower band).

(E) Knockdown of SRPK1 switches VEGF splicing. RT-PCR of RNA extracted from *DDS* podocytes transfected with three different siRNAs to SRPK1, or scrambled siRNA (scr). VEGF$_{165}$b or VEGF$_{165}$ cDNA is used as a positive control.

(F) SRPK1 inhibition is antiangiogenic. Normal or *DDS* cells were suspended in matrigel with or without SRPIN340 and implanted into nude mice. Matrigel was excised and photographed. The intensity of red haemoglobin was measured.

(G) RNA was extracted from the matrigel plugs and endothelial content was estimated from VEGFR2 expression level assessed by qRT-PCR. Bar charts are mean ± SEM. See also Figure S3.

VEGF$_{165}$b isoform expression. Treatment of *DDS* podocytes with SRPIN340 resulted in splicing to the distal splice site (VEGF$_{165}$b expression). SRPIN340 exerts 80% inhibition of SRPK2 at 10 μM, but inhibits only one other of 140 serine threonine kinases at that dose by more than 50% (ALK, 71%) (Fukuhara et al., 2006). To confirm that the switch in splicing was due to an effect on SRPK1, three different siRNAs specific for SRPK1 were used. qPCR showed that these inhibited SRPK1 expression to 35 ± 6, 34 ± 11, and 31 ± 16% of scrambled siRNA for siRNA 9, 10, and 11, respectively. This was confirmed by western blotting (Figure S3B). This compares with 20.5% SRPK1 mRNA expression in the WT1 transfected *DDS* podocytes. Figure 3E shows that all three siRNAs resulted in VEGF$_{165}$b expression in the *DDS* podocytes. To ensure that the siRNAs were not acting through off-target effects, an SRPK1 construct was generated that was insensitive to siRNA9. Transfection of this into the siRNA9 transfected cells restored *DDS* VEGF expression, inhibiting VEGF$_{165}$b and favoring proximal splicing (Figure S3C). qPCR of SRPK2, a related splice-factor kinase, showed no change in *DDS* cells compared with normal podocytes and was not affected by SRPK1 knockdown. To determine whether the SRPK1 inhibition resulted in a functional alteration of VEGF production, podocytes were used in a matrigel angiogenesis assay (Figure 3F). When implanted into nude mice, normal podocytes induced little angiogenesis, as seen by mostly clear matrigel plugs. In contrast *DDS* cells resulted in vascularized plugs (Figure 3F, lower). In contrast, when *DDS* cells were treated with SRPIN340, the vascularization was inhibited. To quantify vascularization, qPCR for mouse VEGFR2 was carried out and quantitated relative to a standard curve (Figure S3D). Figure 3G shows that *DDS* podocytes induced more endothelialization of the plugs than did normal podocytes and that this was reversed by SRPIN340 treatment.

WT1 Binds the *SRPK1* Promoter

To identify whether WT1 interacted directly with the *SRPK1* promoter, we used chromatin immunoprecipitation (ChIP) to determine whether WT1 could bind to the promoter region of the *SRPK1* gene. Figure 4A shows a diagram of the *SRPK1* gene and a putative WT1 binding site (similar to the GC-rich EGR consensus) close to the putative transcription start site. Podocytes were subjected to nuclear extraction of the chromatin/protein complex, followed by shearing of the DNA with sonication to generate fragments 200–1000 bp long. This was then subjected to immunoprecipitation with an anti-WT1 antibody, and the precipitate was subjected to PCR using primers across the transcriptional start. In LNCaP prostate cancer cells overexpressing WT1, binding of WT1 to the *VEGF* promoter has been seen in vitro (Graham et al., 2006). To determine whether, in podocytes, WT1 also bound the *VEGF* promoter, the precipitate was subjected to amplification of the *VEGF* promoter in the same region. Primers to the *GAPDH* promoter were used as a negative control. As a positive control, chromatin was immunoprecipitated with an antibody to RNA polymerase II. Figure 4B shows that the *SRPK1* promoter sequence around the transcriptional start site was precipitated with WT1 in normal podocytes and rescued podocytes, but not in *DDS* podocytes. In contrast, WT1 did not bind either the *VEGF* or the *GAPDH*

promoters in either *DDS* or normal podocytes. To determine whether the putative WT1 binding site was functional in the *SRPK1* promoter, a 1661-bp genomic fragment containing the proposed transcriptional start site was cloned into a Luciferase/Renilla reporter gene. The Renilla is under control of the hTK promoter and acts as an expression control. The open bars in Figure 4C show that the ratio of Luciferase to Renilla was almost four times greater in *DDS* podocytes than in normal podocytes, but this ratio was reduced in the rescued *DDS* podocytes. Figure S4A shows that luciferase expression was increased in all three *DDS* cell lines, R336C, M342R, and G349C, compared with normal podocytes. To identify whether the site of repression was located at the 10-bp WT1-binding consensus sequence, this sequence was mutated (Figure 4C). This increased luciferase expression in the normal and rescued podocytes, but it did not significantly affect expression in any of the *DDS* podocyte types (Figure 4C; Figure S4A), as the mutant WT1 protein in these cells is unable to repress SRPK1 expression. However, there was a trend in the three *DDS* cell lines toward reduced expression in the mutated reporters compared to the wild-type. Therefore, to exclude the possibility of other transcription-factor binding sites affecting expression, a shorter (484-bp) sequence was used (Figure S4B). Again, *DDS* cells had a higher luciferase expression than did normal and rescued cells, and when the WT1 binding site was mutated, luciferase expression in normal and rescued cells was again increased, although not to the levels seen in *DDS* cells (Figure S4C). We therefore cannot rule out the possibility that additional regulators in the promoter region interact with the mutated *DDS* protein, but it is clear that the mutant WT1 protein results in elevated SRPK1 expression, at least in part through lack of binding to the WT1 consensus binding sequence. To determine whether the *SRPK1* promoter was inhibited by exogenous WT1, HeLa cells were transfected with the luciferase reporter gene with or without wild-type WT1. Figure 4D shows that transfection of HeLa cells with wild-type WT1 resulted in a significant inhibition of luciferase expression to ∼30% of that in cells not transfected with WT1. Figure 4E shows that this repression of the normal *SRPK1* promoter by wild-type WT1 to 31 ± 6% was significantly lifted by the use of the WT1 binding site mutant SRPK1 promoter (WTBSmut, 63 ± 6%), but again not to 100%, so additional regulators may be active.

SRPK1 Is Upregulated and SRSF1 Is Localized to Nuclei in Human *DDS*

To determine whether the upregulation of SRPK1 was also seen in human *DDS* patients in vivo, RNA was extracted from paraffin-embedded sections of renal cortex from five patients with Denys Drash Syndrome or five histologically normal kidney sections. Figure 4F shows that SRPK1 was significantly greater (4.3 ± 1.2-fold, p < 0.01, one sample t test) relative to GAPDH in the *DDS* patients. To determine whether SRSF1 was relocated from the cytoplasm, sections were stained with SRSF1 antibody. Although there was no difference in tubular staining of SRSF1 between normal and *DDS* patients, in the glomeruli in the normal kidneys there was substantial podocyte cytoplasmic staining (Figure 4G, left, arrows), whereas in the glomeruli of *DDS* patients, staining appeared to be more localized to the nuclei of the podocytes (Figure 4G, right, arrows).
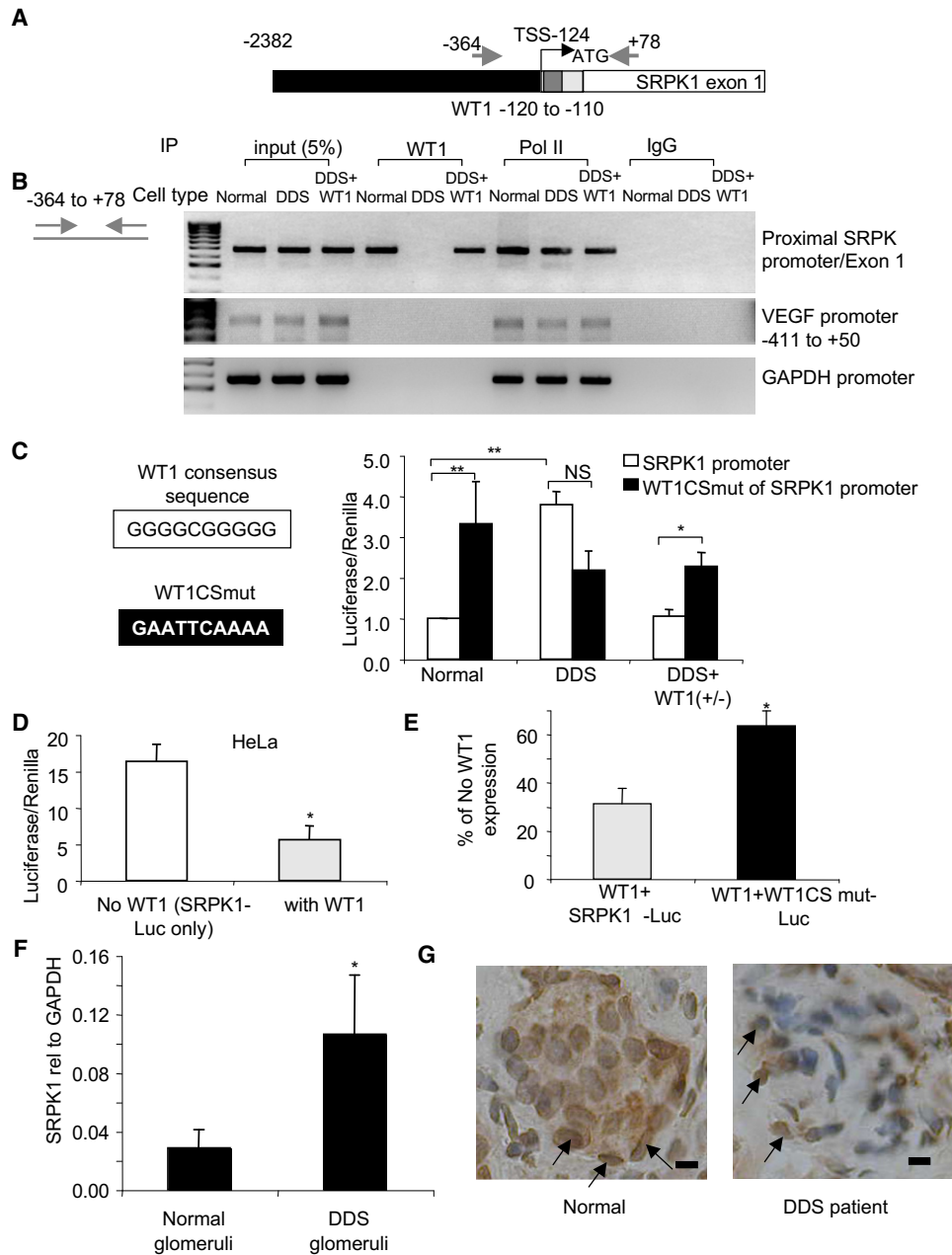
Figure 4. WT1 Represses SRPK1 Expression by Binding the SRPK1 Promoter Region

(A) SRPK1 gene structure. Black, promoter region; gray, WT1 binding site; silver, 5′UTR; white, coding sequence of exon 1. Arrows indicate primer locations. Numbers are bp relative to the start codon.

(B) WT1 binds the SRPK1 promoter. Nuclear extracts from podocytes were sheared to fragment DNA, immunoprecipitated with polymerase II antibody, human IgG, or a WT1 antibody, and subjected to PCR using primers to detect the region around the SRPK1 transcriptional start site (TSS) or the VEGF or GAPDH promoters.

(C) DDS mutations relieve SRPK1 repression. Podocytes were transfected with an SRPK1 promoter-luciferase reporter vector (white bars), or the same promoter with a 10-bp mutation of the WT1 consensus sequence (WT1CSmut; black bars).

(D) WT1 represses SRPK1 expression. HeLa cells were transfected with the wild-type promoter reporter gene alone (open bars) or also with WT1 (silver bars), and bioluminescence was measured.

(E) The 10-bp consensus sequence adjacent to the TSS is responsible for part of the repression. HeLa cells transfected with WT1 and the wild-type SRPK1 promoter (silver bars) or WT1 and the mutated SRPK1 promoter (black bars). Luciferase/Renilla is expressed as a percentage of bioluminescence in the absence of WT1 (white bar in D).

(F) qPCR of SRPK1 RNA from histologically normal kidney (n = 5) or children with *DDS* (n = 5, p < 0.05). Bar charts are mean ± SEM.

(G) Immunohistochemistry for SRSF1 of kidney biopsies of *DDS* subjects (right) compared with normal subjects (left). Podocytes are shown by arrows. Scale bar = 15 μm. See also Figure S4.

SRPK1 Inhibition Inhibits Angiogenesis

To determine whether the proangiogenic VEGF isoform expression due to SRPK1 is necessary for angiogenesis, we employed a widely used model of choroidal neovascularization that is amenable to local administration of pharmacological tools. Treatment of epithelial cells with 10 μM SRPIN340 resulted in an increase in VEGF$_{165}$b expression (Nowak et al., 2010). In a mouse model of choroidal neovascularization 3 days after treatment with SRPIN340 (10 pmol/eye), the ratio of total VEGF (containing exon 2/3) to proangiogenic isoforms (containing exon 8a) was significantly greater than in saline-treated controls (Figure 5A), as determined by qPCR. Two weeks after SRPIN340 treatment, there was a substantial and significant inhibition of fluorescein leakage (Figure 5B) and lesion size (Figure 5C) in the SRPIN340-treated mice compared with both controls and mice treated with eye injection with an inhibitor of a closely related kinase, Clk1/4 (TG003). The inhibition of angiogenesis was similar to that seen with recombinant VEGF$_{165}$b protein (Hua et al., 2010). To determine whether the inhibition of splicing to VEGF$_{165}$ was sufficient to inhibit tumor growth and angiogenesis, LS174t colorectal tumor cells, the growth of which has previously been shown to be inhibited by the antiangiogenic actions of VEGF$_{165}$b, were stably transfected with an SRPK1-shRNAi lentiviral vector. Stable cell lines (Figure S5A) were generated and SRPK1 levels were measured by qPCR. These were knocked down by 96% (Figure S5B). SRPK1 knockdown cells grew at the same rate as the scrambled shRNAi cells. To determine whether SRPK1 knockdown affected VEGF splicing, RNA and protein were extracted and subjected to RT-PCR and ELISA, respectively. SRPK1 shRNAi-expressing cells showed stronger expression of VEGF$_{165}$b mRNA (Figure 5D) and VEGF$_{165}$b protein in the cell (Figure S5C) and the media (Figure S5D). To determine whether the SRPK1 knockdown resulted in a functional alteration of VEGF, cells were transfected with SRPK1 shRNAi lentivirus, and media collected for in vitro angiogenesis assays. Media from untransfected cells stimulated endothelial cell tube formation on fibroblasts, but media from SRPK1 shRNAi-transfected cells had no effect (Figure 5E). These tumor cells were then implanted into nude mice and the tumor growth rate was measured. The SRPK1 shRNAi cells formed smaller tumors than did the scrambled shRNAi controls, and the tumors grew more slowly (Figure 5F). Staining of these cells for microvascular density by VEGFR2 immunofluorescence showed significantly lower density for SRPK1 shRNAi cells than for scrambled controls (Figure 5G).

DISCUSSION

These results indicate a link between the physiological role of an important tumor suppressor gene (*WT1*) and regulation of the angiogenic or antiangiogenic properties of VEGF and other genes by alternative splicing. There have been many studies identifying alternative splicing as a process that regulates oncogenesis. For instance, a splice variant of p53 (p47) is an N-terminally deleted form of p53 and inhibits its tumor suppressor activity (Ghosh et al., 2004), and a correlation was seen between inactive p53 isoforms and VEGF$_{165}$b splicing in colorectal cancers (Díaz et al., 2008). However, in this case as in many others, it is the tumor suppressor gene itself that is alternatively spliced to give different isoforms. It is less common to find a link between a tumor suppressor gene and a tumor regulatory process that involves alternative splice-site regulation. One such example is the regulation of alternative Fas splicing by RBM5, whereby RBM5 binds to U2AF[65] and prevents inclusion of exon 6 of Fas. Thus, the tumor suppressor gene acts by directly interacting with the spliceosome (Bonnal et al., 2008). Other tumor-mediated pathways have also been implicated; for instance, Ras increases alternative splicing of KLF6, a tumor suppressor gene in colorectal cancer, through PI3K and Akt, and through a mechanism that is also SRSF1 mediated, suggesting that Akt-mediated phosphorylation of SRSF1 is also sufficient to alter splicing of the tumor suppressor gene itself (Yea et al., 2008). The data presented here go one step further and demonstrate the mechanism by which a mutation in a known tumor suppressor gene causes a change in a splicing process that results in alternative splicing of other genes that contribute to tumor progression (in this case by angiogenesis). As WT1 is implicated in renal disease, gonadal development, and in several cancers, the mechanistic link between WT1 expression (including WT1 splice variants), SRPK1 expression, and SRSF1 activity will be of significant interest. It had previously been shown that WT1 could modify splicing and interact directly with splicing proteins, for instance by binding U2AF65, but this interaction required the KTS sequence (Davies et al., 1998). The finding that only the isoforms lacking the KTS domain (and hence non-RNA binding) repress SRPK1 expression provides another mechanism through which WT1 can alter RNA processing: transcriptional repression of a splicing-factor kinase. Thus, one of the consequences of misexpression of WT1 in tumors is an altered pattern of alternative splicing of key cancer-associated genes (including VEGF), not only through direct interaction with splicing factors (Davies et al., 1999), but also through controlled expression of splice-factor kinases.

The upregulation of SRPK1 expression by *WT1* mutants (and hence suppression of SRPK1 by wild-type WT1) indicates that SRPK1 upregulation may be a common cancer-related event. It has been shown that SRPK1 is upregulated in pancreatic, breast, and colon carcinomas (Hayes et al., 2007), but is reduced in neuroblastoma (and this correlates with drug resistance) (Krishnakumar et al., 2008). This is consistent with studies showing that in tumor cells, the target for SRPK1, SRSF1, is phosphorylated and located in the nucleus (Sanford et al., 2005), as seen in this study in HeLa cells but not in HEK293T cells (an epithelial cell line that is not tumorigenic). Thus, nuclear SRSF1 may be more common in cultured cancer cells than in differentiated cells, a hypothesis that needs to be tested. It indicates that phosphorylated, nuclear SRSF1 is indicative of an angiogenic phenotype in that it results in proximal splicing and production of angiogenic VEGF isoforms. This is supported by work showing that IGF-mediated PKC activation induces binding of phosphorylated SRSF1 to the VEGF pre-mRNA (Nowak et al., 2010). However, this is evidence that upregulation of SRPK1 is by a specific mechanism. It also identifies a link between WT1 and a putative mechanism for the glomerular dysfunction of *DDS*, proposed by Schumacher et al. to be mediated by alternative VEGF splicing (Schumacher et al., 2007), and for which there is indirect evidence from overexpression of *WT1* mutants in
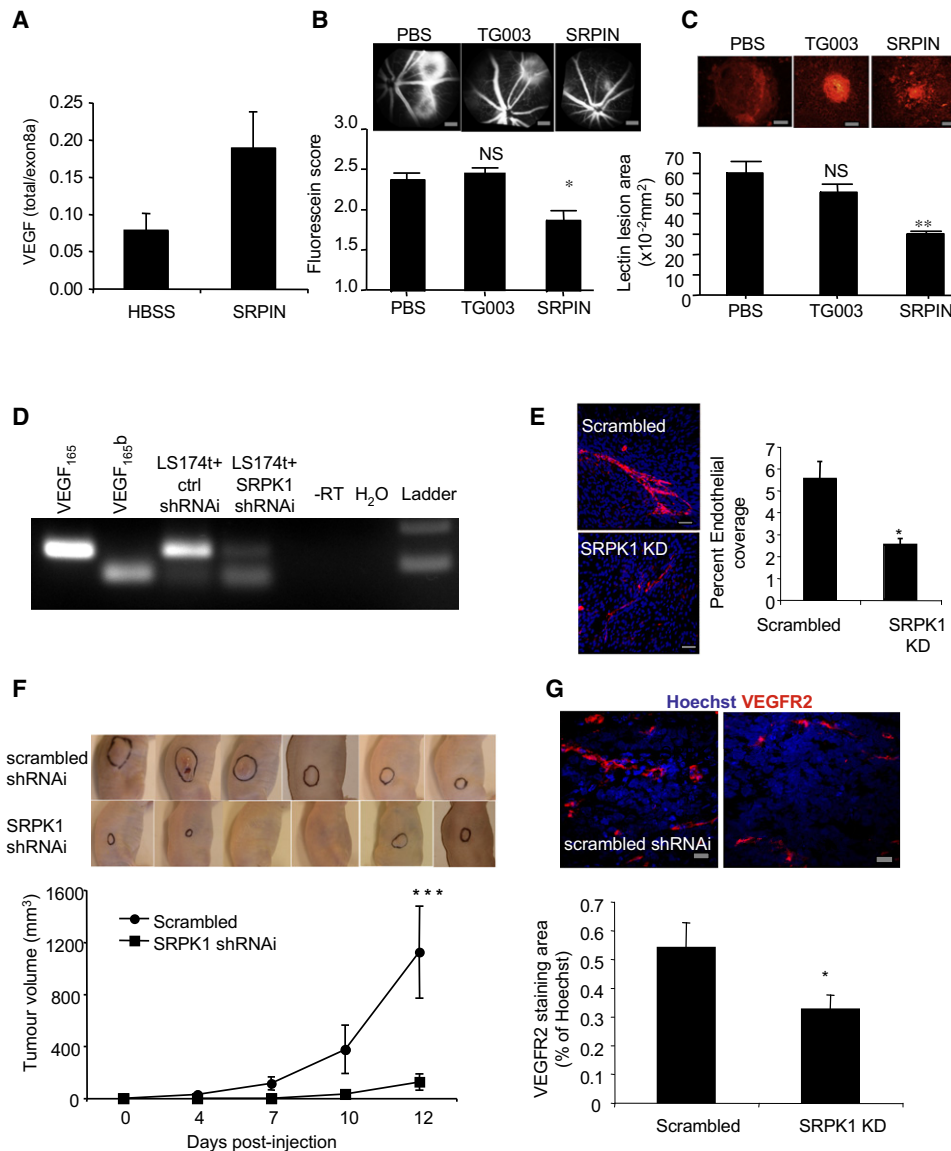
Figure 5. SRPK1 Inhibition is Antiangiogenic

(A) Mice underwent laser photocoagulation and were treated with SRPIN340 (inhibits SRPK1, n = 24), TG003 (inhibits Clk1/4, n = 18), or vehicle (n = 24). Two to three days later, six HBSS-treated and six SRPIN340-treated mice were killed, their eyes were enucleated, and their RNA was extracted and subjected to qRT-PCR for total VEGF (primers in exon 3) or exon-8a-containing VEGF (e.g., $VEGF_{164}$).

(B) The remaining mice were treated again 7 days later with the compounds and then, after another 7 days, subjected to fluorescein angiography. Lesion size was scored blind. Scale bar = 300 μm.

(C) The mice were then killed and their retinal membranes flat-mounted and stained for lectin to identify choroidal angiogenesis (red). The size of the lesions was measured. **p < 0.01, *p < 0.05 compared with PBS, ANOVA. Scale bar = 100 μm.

(D) LS174t colon cancer cells were infected with lentivirus containing SRPK1-shRNAi or scrambled siRNA (ctrl) and selected with puromycin. Stable cell lines were subjected to RT-PCR for $VEGF_{165}$b and $VEGF_{165}$ levels.

(E) Knockdown of SRPK1 reduces the angiogenic potential of media. Cells were infected with SRPK1 shRNAi and the media collected. Media was used in an in vitro coculture assay of endothelial cells and fibroblasts, and cells stained for CD31 (red, endothelial) and Hoechst (nuclei). Spread of endothelial cells was determined by measuring the ratio of area covered by CD31 staining relative to that covered by Hoechst staining. **p < 0.01. Scale bar = 200 μm.

(F) Tumor cells were implanted into nude mice and tumors allowed to grow for 12 days. Tumors are outlined in black. Tumour diameters were measured by callipers. ***p < 0.001 by two way ANOVA.

(G) Tumors were excised and stained for VEGFR2 (red) and Hoechst (blue) and vessel density was determined by VEGFR2 staining relative to Hoechst. *p < 0.05 compared with scrambled siRNA, t test. Scale bar = 20 μm. Bar charts are mean ± SEM. See also Figure S5.

transgenic mice in which abnormalities in glomerular capillaries are postulated to be caused by altered VEGF function (Natoli et al., 2002).

We recently showed that neonatal retinal neovascularization induced by hyperoxia is reduced by SRPIN340 treatment (Nowak et al., 2010). We have now extended these findings by

showing that SRPK1 inhibition is effective in tumor models of cancers that are treated by anti-VEGF therapy. The substantial inhibition of angiogenesis coupled with reduced lesion size demonstrates that interfering with VEGF splicing mechanisms is a rational target for antiangiogenic therapy in tumors. In particular, it suggests that angiogenesis may be driven in tumors that lack functional WT1 (exemplified by LS174t cells), or have enhanced SRPK1 expression (Koesters et al., 2004), by control of VEGF splicing rather than (or as well as) control of VEGF expression. This has implications for the rational use of anti-VEGF agents, as VEGF inhibitors have been shown to be ameliorated in the presence of increased $VEGF_{165}b$ expression (Varey et al., 2008).

These results provide a potential mechanism for a different antiangiogenic therapeutic approach (specifically, the inhibition of SRPK1), and they also identify SRSF1 localization as a possible rational diagnostic marker for WT1 dysfunction in the context of angiogenesis. Alternative splicing of several other cancer-associated genes may also be affected through WT1's ability to regulate SRPK1.

EXPERIMENTAL PROCEDURES

Human Samples and Ethics
All human samples were anonymized and experiments were approved by the North Bristol Ethics Committee (Southmead Hostpital) number 07/H0102/45.

Cell Culture and Transfection
Specific details of the experimental procedures are given in the online supplement.

The conditionally immortalized podocytes used were from a healthy individual and from three patients suffering from Denys Drash Syndrome (R336C, M342R, and G349C). After growing to the required confluence, the podocytes were thermoswitched at 37°C for 14 days to ensure growth arrest and differentiation. Both podocyte cell types (DDS and normal) were used at the same stage of differentiation (14 days thermoswitched).

Protein Studies: Immunoblotting and Immunoprecipitation
Both whole-cell lysate (nuclear and cytoplasmic) protein extraction and nuclear protein extracts were used as described in the online supplement. The extracts were then immunoblotted using either mouse anti-SRPK1 (anti-SRPK1; BD 611072; 1:1000), rabbit anti-panVEGF (Santa Cruz A20 sc-152; 1:500), mouse anti-VEGF$_{xxx}$b (MAB3045; R&D; 1:500), goat anti-SRSF1 (SC10255; 1:500), mouse anti-SRSF1 (AK96) (Santa Cruz SC-33562), or rabbit anti-GAPDH (Sigma G9545, 1:2000). For immunoprecipitation phospho-SRSF1 studies, cell lysates were incubated with mouse anti-SRSF1 (Santa Cruz SC-33562) or anti-Pan-phospho-SR antibody (Santa Cruz SC-13509) and Protein G Dynabeads (Invitrogen). To detect phosphorylated SRSF1, the eluent was immunoblotted with either anti-SRSF1 or the anti-Pan-phospho-SR antibody (1:500).

ELISA
A pan-VEGF capture antibody (Duoset VEGF ELISA DY-293; R&D Systems) and recombinant human $VEGF_{165}$ or $VEGF_{165}b$ standards were used. Biotinylated goat anti-human VEGF (0.025 μg/ml; R&D Systems) or mouse anti-human $VEGF_{165}b$ (clone 264610/1, 0.025 μg/ml, R&D Systems) were used as detection antibodies. Details are given in the online supplement.

Semiquantitative PCR and qPCR
mRNA was extracted from differentiated podocytes using standard methodology, given in the online supplement. To extract RNA from paraffin-embedded DDS kidneys (n = 5) and paraffin-embedded non-WT1 child kidneys (n = 5), two sections of 6 μm thickness were used from each. RNA was then extracted using RNeasy FFPE kit (QIAGEN). RT-PCR was performed

to differentiate between exon-8a- and exon-8b-containing isoforms within the same sample in the same reaction using primers specific to exon 7a and the 3′ untranslated region of the VEGF gene (Nowak et al., 2008). For qPCR, 1% of the cDNA from the cell lines was used per reaction, whereas 5% of the cDNA from paraffin-embedded sections was used. The qPCR reaction was set up using Roche SyBr Green and run in an ABI 7000. Validated primers specific to SRPK1, SRSF1, and GAPDH were used for the qPCR.

Chromatin Immunoprecipitation
ChIP was performed on the differentiated podocytes using the Imprint ChIP Kit (Sigma). Cells were incubated with 1% formaldehyde to crosslink DNA to protein. The cells were then lysed and DNA sheared to about 1000 bp using a sonicator. The DNA-protein mixture, incubated with WT1, polymerase II antibody, or nonspecific IgG, was immunoprecipitated, and the crosslinked DNA-WT1 complex was released using proteinase K, after which the DNA was cleaned up and eluted using GeneElute Binding Column (Sigma) and the eluted DNA was subjected to PCR to detect SRPK1, VEGF, and GAPDH promoter regions.

Luciferase Assays
A 1661-bp fragment and a 484-bp fragment containing the upstream promoter sequence of SRPK1 were amplified from genomic DNA and cloned into pGL3, as described in the online supplement, to generate the wild-type SRPK1 promoter. The SRPK1 promoter sequence was verified by restriction analysis and sequencing. The putative WT1 binding site located −119 bp to −110 bp upstream of the SRPK1 start codon was mutated from GGGGCGGGGG to GAATTCAAAA as described in the online supplement.

Animal Experiments
All animal experiments were approved by the University of Southern California (USC) Animal Use Committee (ocular experiments), or under license by the UK Home Office and in accordance with the University of Bristol ethical review panel (tumor experiments).

Induction of Choroidal Neovascularization
Details are given in the online supplement. C56Bl/6J mice were anesthetized by intraperitoneal injection of ketamine and xylazine hydrochloride. Four photocoagulation lesions were delivered with a diode green laser between the retinal vessels 1–2 disc diameters apart in each eye. Two μl of saline, 10 ng $rhVEGF$-$A_{165}b$, 100 pmol SRPIN340, or 100 pmol TG003 was injected into the vitreous immediately after photocoagulation and 7 days later. Fourteen days after laser treatment, fluorescein angiography of the fundi was carried out, and the animals were sacrificed after imaging. Eyes were enucleated and fixed. Three animals given SRPIN340 or saline were sacrificed 3 days after photocoagulation, and RNA was extracted for qPCR.

Tumor Studies
LS174t colorectal tumor cells were infected with lentiviral SRPK1 shRNAi or standard and selected with puromycin. Cells were checked for positive expression by GFP (Figure S5A). SRPK1 knockdown was assessed by qPCR as above. VEGF was assessed as above using a $VEGF_{165}b$-specific ELISA (see Methods in the Supplemental Information), and a pan VEGF ELISA. The difference was used to calculate $VEGF_{165}$.

SUPPLEMENTAL INFORMATION

Supplemental Information includes five figures and Supplemental Experimental Procedures and can be found with this article online at doi:10.1016/j.ccr.2011.10.016.

REFERENCES

Artac, R.A., McFee, R.M., Smith, R.A., Baltes-Breitwisch, M.M., Clopton, D.T., and Cupp, A.S. (2009). Neutralization of vascular endothelial growth factor antiangiogenic isoforms is more effective than treatment with proangiogenic isoforms in stimulating vascular development and follicle progression in the perinatal rat ovary. Biol. Reprod. 81, 978–988.

Ballmer-Hofer, K., Andersson, A.E., Ratcliffe, L.E., and Berger, P. (2011). Neuropilin-1 promotes VEGFR-2 trafficking through Rab11 vesicles thereby specifying signal output. Blood 118, 816–826.

Baltes-Breitwisch, M.M., Artac, R.A., Bott, R.C., McFee, R.M., Kerl, J.G., Clopton, D.T., and Cupp, A.S. (2010). Neutralization of vascular endothelial growth factor antiangiogenic isoforms or administration of proangiogenic isoforms stimulates vascular development in the rat testis. Reproduction 140, 319–329.

Bates, D.O., Cui, T.G., Doughty, J.M., Winkler, M., Sugiono, M., Shields, J.D., Peat, D., Gillatt, D., and Harper, S.J. (2002). VEGF165b, an inhibitory splice variant of vascular endothelial growth factor, is down-regulated in renal cell carcinoma. Cancer Res. 62, 4123–4131.

Blann, A.D., Li, J.L., Li, C., and Kumar, S. (2001). Increased serum VEGF in 13 children with Wilms' tumour falls after surgery but rising levels predict poor prognosis. Cancer Lett. 173, 183–186.

Bonnal, S., Martínez, C., Förch, P., Bachi, A., Wilm, M., and Valcárcel, J. (2008). RBM5/Luca-15/H37 regulates Fas alternative splice site pairing after exon definition. Mol. Cell 32, 81–95.

Bor, Y.C., Swartz, J., Morrison, A., Rekosh, D., Ladomery, M., and Hammarskjöld, M.L. (2006). The Wilms' tumor 1 (WT1) gene (+KTS isoform) functions with a CTE to enhance translation from an unspliced RNA with a retained intron. Genes Dev. 20, 1597–1608.

Cébe Suarez, S., Pieren, M., Cariolato, L., Arn, S., Hoffmann, U., Bogucki, A., Manlius, C., Wood, J., and Ballmer-Hofer, K. (2006). A VEGF-A splice variant defective for heparan sulfate and neuropilin-1 binding shows attenuated signaling through VEGFR-2. Cell. Mol. Life Sci. 63, 2067–2077.

Davies, R., Moore, A., Schedl, A., Bratt, E., Miyahawa, K., Ladomery, M., Miles, C., Menke, A., van Heyningen, V., and Hastie, N. (1999). Multiple roles for the Wilms' tumor suppressor, WT1. Cancer Res. 59, 1747s–1750s; discussion 1751s.

Davies, R.C., Calvio, C., Bratt, E., Larsson, S.H., Lamond, A.I., and Hastie, N.D. (1998). WT1 interacts with the splicing factor U2AF65 in an isoform-dependent manner and can be incorporated into spliceosomes. Genes Dev. 12, 3217–3225.

Denys, P., Malvaux, P., Van Den Berghe, H., Tanghe, W., and Proesmans, W. (1967). [Association of an anatomo-pathological syndrome of male pseudo-hermaphroditism, Wilms' tumor, parenchymatous nephropathy and XX/XY mosaicism]. Arch. Fr. Pediatr. 24, 729–739.

Díaz, R., Peña, C., Silva, J., Lorenzo, Y., García, V., García, J.M., Sánchez, A., Espinosa, P., Yuste, R., Bonilla, F., and Domínguez, G. (2008). p73 Isoforms affect VEGF, VEGF165b and PEDF expression in human colorectal tumors: VEGF165b downregulation as a marker of poor prognosis. Int. J. Cancer 123, 1060–1067.

Drash, A., Sherman, F., Hartmann, W.H., and Blizzard, R.M. (1970). A syndrome of pseudohermaphroditism, Wilms' tumor, hypertension, and degenerative renal disease. J. Pediatr. 76, 585–593.

Fukuhara, T., Hosoya, T., Shimizu, S., Sumi, K., Oshiro, T., Yoshinaka, Y., Suzuki, M., Yamamoto, N., Herzenberg, L.A., Herzenberg, L.A., and

Hagiwara, M. (2006). Utilization of host SR protein kinases and RNA-splicing machinery during viral replication. Proc. Natl. Acad. Sci. USA 103, 11329–11333.

Ghosh, A., Stewart, D., and Matlashewski, G. (2004). Regulation of human p53 activity and cell localization by alternative splicing. Mol. Cell. Biol. 24, 7987–7997.

Gonçalves, V., Matos, P., and Jordan, P. (2009). Antagonistic SR proteins regulate alternative splicing of tumor-related Rac1b downstream of the PI3-kinase and Wnt pathways. Hum. Mol. Genet. 18, 3696–3707.

Graham, K., Li, W., Williams, B.R., and Fraizer, G. (2006). Vascular endothelial growth factor (VEGF) is suppressed in WT1-transfected LNCaP cells. Gene Expr. 13, 1–14.

Haber, D.A., Sohn, R.L., Buckler, A.J., Pelletier, J., Call, K.M., and Housman, D.E. (1991). Alternative splicing and genomic structure of the Wilms tumor gene WT1. Proc. Natl. Acad. Sci. USA 88, 9618–9622.

Harper, S.J., and Bates, D.O. (2008). VEGF-A splicing: the key to anti-angiogenic therapeutics? Nat. Rev. Cancer 8, 880–887.

Hayes, G.M., Carrigan, P.E., and Miller, L.J. (2007). Serine-arginine protein kinase 1 overexpression is associated with tumorigenic imbalance in mitogen-activated protein kinase pathways in breast, colonic, and pancreatic carcinomas. Cancer Res. 67, 2072–2080.

Hohenstein, P., and Hastie, N.D. (2006). The many facets of the Wilms' tumour gene, WT1. Hum. Mol. Genet. 15 (Spec No 2), R196–R201.

Houck, K.A., Ferrara, N., Winer, J., Cachianes, G., Li, B., and Leung, D.W. (1991). The vascular endothelial growth factor family: identification of a fourth molecular species and characterization of alternative splicing of RNA. Mol. Endocrinol. 5, 1806–1814.

Hua, J., Spee, C., Kase, S., Rennel, E.S., Magnussen, A.L., Qiu, Y., Varey, A., Dhayade, S., Churchill, A.J., Harper, S.J., et al. (2010). Recombinant human VEGF165b inhibits experimental choroidal neovascularization. Invest. Ophthalmol. Vis. Sci. 51, 4282–4288.

Hurwitz, H., Fehrenbacher, L., Novotny, W., Cartwright, T., Hainsworth, J., Heim, W., Berlin, J., Baron, A., Griffing, S., Holmgren, E., et al. (2004). Bevacizumab plus irinotecan, fluorouracil, and leucovorin for metastatic colorectal cancer. N. Engl. J. Med. 350, 2335–2342.

Karni, R., de Stanchina, E., Lowe, S.W., Sinha, R., Mu, D., and Krainer, A.R. (2007). The gene encoding the splicing factor SF2/ASF is a proto-oncogene. Nat. Struct. Mol. Biol. 14, 185–193.

Kawamura, H., Li, X., Harper, S.J., Bates, D.O., and Claesson-Welsh, L. (2008). Vascular endothelial growth factor (VEGF)-A165b is a weak in vitro agonist for VEGF receptor-2 due to lack of coreceptor binding and deficient regulation of kinase activity. Cancer Res. 68, 4683–4692.

Koesters, R., Linnebacher, M., Coy, J.F., Germann, A., Schwitalle, Y., Findeisen, P., and von Knebel Doeberitz, M. (2004). WT1 is a tumor-associated antigen in colon cancer that can be recognized by in vitro stimulated cytotoxic T cells. Int. J. Cancer 109, 385–392.

Konopatskaya, O., Churchill, A.J., Harper, S.J., Bates, D.O., and Gardiner, T.A. (2006). VEGF165b, an endogenous C-terminal splice variant of VEGF, inhibits retinal neovascularization in mice. Mol. Vis. 12, 626–632.

Krishnakumar, S., Mohan, A., Kandalam, M., Ramkumar, H.L., Venkatesan, N., and Das, R.R. (2008). SRPK1: a cisplatin sensitive protein expressed in retinoblastoma. Pediatr. Blood Cancer 50, 402–406.

Manetti, M., Guiducci, S., Romano, E., Ceccarelli, C., Bellando-Randone, S., Conforti, M.L., Ibba-Manneschi, L., and Matucci-Cerinic, M. (2011). Overexpression of VEGF165b, an inhibitory splice variant of vascular endothelial growth factor, leads to insufficient angiogenesis in patients with systemic sclerosis. Circ. Res. 109, e14–e26.

Merdzhanova, G., Gout, S., Keramidas, M., Edmond, V., Coll, J.L., Brambilla, C., Brambilla, E., Gazzeri, S., and Eymin, B. (2010). The transcription factor E2F1 and the SR protein SC35 control the ratio of pro-angiogenic versus antiangiogenic isoforms of vascular endothelial growth factor-A to inhibit neovascularization in vivo. Oncogene 29, 5392–5403.

Morrison, A.A., Viney, R.L., and Ladomery, M.R. (2008). The post-transcriptional roles of WT1, a multifunctional zinc-finger protein. Biochim. Biophys. Acta 1785, 55–62.

Natoli, T.A., Liu, J., Eremina, V., Hodgens, K., Li, C., Hamano, Y., Mundel, P., Kalluri, R., Miner, J.H., Quaggin, S.E., and Kreidberg, J.A. (2002). A mutant form of the Wilms' tumor suppressor gene WT1 observed in Denys-Drash syndrome interferes with glomerular capillary development. J. Am. Soc. Nephrol. 13, 2058–2067.

Nowak, D.G., Woolard, J., Amin, E.M., Konopatskaya, O., Saleem, M.A., Churchill, A.J., Ladomery, M.R., Harper, S.J., and Bates, D.O. (2008). Expression of pro- and anti-angiogenic isoforms of VEGF is differentially regulated by splicing and growth factors. J. Cell Sci. 121, 3487–3495.

Nowak, D.G., Amin, E.M., Rennel, E.S., Hoareau-Aveilla, C., Gammons, M., Damodoran, G., Hagiwara, M., Harper, S.J., Woolard, J., Ladomery, M.R., and Bates, D.O. (2010). Regulation of vascular endothelial growth factor (VEGF) splicing from pro-angiogenic to anti-angiogenic isoforms: a novel therapeutic strategy for angiogenesis. J. Biol. Chem. 285, 5532–5540.

Perrin, R.M., Konopatskaya, O., Qiu, Y., Harper, S., Bates, D.O., and Churchill, A.J. (2005). Diabetic retinopathy is associated with a switch in splicing from anti- to pro-angiogenic isoforms of vascular endothelial growth factor. Diabetologia 48, 2422–2427.

Qiu, Y., Bevan, H., Weeraperuma, S., Wratting, D., Murphy, D., Neal, C.R., Bates, D.O., and Harper, S.J. (2008). Mammary alveolar development during lactation is inhibited by the endogenous antiangiogenic growth factor isoform, VEGF165b. FASEB J. 22, 1104–1112.

Qiu, Y., Ferguson, J., Oltean, S., Neal, C.R., Kaura, A., Bevan, H., Wood, E., Sage, L.M., Lanati, S., Nowak, D.G., et al. (2010). Overexpression of VEGF165b in podocytes reduces glomerular permeability. J. Am. Soc. Nephrol. 21, 1498–1509.

Rennel, E., Waine, E., Guan, H., Schüler, Y., Leenders, W., Woolard, J., Sugiono, M., Gillatt, D., Kleinerman, E., Bates, D., and Harper, S. (2008). The endogenous anti-angiogenic VEGF isoform, VEGF165b inhibits human tumour growth in mice. Br. J. Cancer 98, 1250–1257.

Rennel, E., Varey, A.H.R., Churchill, A.J., Wheatley, E.R., Stewart, L., Mather, S., Bates, D.O., and Harper, S.J. (2009). VEGF121b, a new member of the VEGFxxxb family of VEGF-A splice isoforms, inhibits neovascularisation and tumour growth in vivo. Br. J. Cancer 101, 1183–1193.

Sanford, J.R., Ellis, J.D., Cazalla, D., and Cáceres, J.F. (2005). Reversible phosphorylation differentially affects nuclear and cytoplasmic functions of splicing factor 2/alternative splicing factor. Proc. Natl. Acad. Sci. USA 102, 15042–15047.

Sanford, J.R., Coutinho, P., Hackett, J.A., Wang, X., Ranahan, W., and Caceres, J.F. (2008). Identification of nuclear and cytoplasmic mRNA targets for the shuttling protein SF2/ASF. PLoS ONE 3, e3369.

Schumacher, V.A., Jeruschke, S., Eitner, F., Becker, J.U., Pitschke, G., Ince, Y., Miner, J.H., Leuschner, I., Engers, R., Everding, A.S., et al. (2007). Impaired glomerular maturation and lack of VEGF165b in Denys-Drash syndrome. J. Am. Soc. Nephrol. 18, 719–729.

Sköldenberg, E.G., Christiansson, J., Sandstedt, B., Larsson, A., Läckgren, G., and Christofferson, R. (2001). Angiogenesis and angiogenic growth factors in Wilms tumor. J. Urol. 165, 2274–2279.

Varey, A.H., Rennel, E.S., Qiu, Y., Bevan, H.S., Perrin, R.M., Raffy, S., Dixon, A.R., Paraskeva, C., Zaccheo, O., Hassan, A.B., et al. (2008). VEGF165b, an antiangiogenic VEGF-A isoform, binds and inhibits bevacizumab treatment in experimental colorectal carcinoma: balance of pro- and antiangiogenic VEGF-A isoforms has implications for therapy. Br. J. Cancer 98, 1366–1379.

Viney, R.L., Morrison, A.A., van den Heuvel, L.P., Ni, L., Mathieson, P.W., Saleem, M.A., and Ladomery, M.R. (2007). A proteomic investigation of glomerular podocytes from a Denys-Drash syndrome patient with a mutation in the Wilms tumour suppressor gene WT1. Proteomics 7, 804–815.

Woolard, J., Wang, W.Y., Bevan, H.S., Qiu, Y., Morbidelli, L., Pritchard-Jones, R.O., Cui, T.G., Sugiono, M., Waine, E., Perrin, R., et al. (2004). VEGF165b, an inhibitory vascular endothelial growth factor splice variant: mechanism of action, in vivo effect on angiogenesis and endogenous protein expression. Cancer Res. 64, 7822–7835.

Woolard, J., Bevan, H.S., Harper, S.J., and Bates, D.O. (2009). Molecular diversity of VEGF-A as a regulator of its biological activity. Microcirculation 16, 572–592.

Yea, S., Narla, G., Zhao, X., Garg, R., Tal-Kremer, S., Hod, E., Villanueva, A., Loke, J., Tarocchi, M., Akita, K., et al. (2008). Ras promotes growth by alternative splicing-mediated inactivation of the KLF6 tumor suppressor in hepatocellular carcinoma. Gastroenterology 134, 1521–1531.

Zhong, X.Y., Ding, J.H., Adams, J.A., Ghosh, G., and Fu, X.D. (2009). Regulation of SR protein phosphorylation and alternative splicing by modulating kinetic interactions of SRPK1 with molecular chaperones. Genes Dev. 23, 482–495.